Coordination Complexes

Deutsche Ausgabe: DOI: 10.1002/ange.201607861
Internationale Ausgabe: DOI: 10.1002/anie.201607861

A Ruthenium(III)–Oxyl Complex Bearing Strong Radical Character

*Yoshihiro Shimoyama, Tomoya Ishizuka, Hiroaki Kotani, Yoshihito Shiota, Kazunari Yoshizawa, Kaoru Mieda, Takashi Ogura, Toshihiro Okajima, Shunsuke Nozawa, and Takahiko Kojima**

Abstract: *Proton-coupled electron-transfer oxidation of a Ru^{II}–OH_2 complex, having an N-heterocyclic carbene ligand, gives a Ru^{III}–$O^{\bullet}$ species, which has an electronically equivalent structure of the Ru^{IV}=O species, in an acidic aqueous solution. The Ru^{III}–$O^{\bullet}$ complex was characterized by spectroscopic methods and DFT calculations. The oxidation state of the Ru center was shown to be close to +3; the Ru–O bond showed a lower-energy Raman scattering at 732 cm^{-1} and the Ru–O bond length was estimated to be 1.77(1) Å. The Ru^{III}–$O^{\bullet}$ complex exhibits high reactivity in substrate oxidation under catalytic conditions; particularly, benzaldehyde and the derivatives are oxidized to the corresponding benzoic acid through C–H abstraction from the formyl group by the Ru^{III}–$O^{\bullet}$ complex bearing a strong radical character as the active species.*

High-valent metal–oxo complexes are an important class of compounds, because they are found as reactive intermediates in oxidation by metalloenzymes and synthetic oxidation reactions.[1,2] In studies on the metal–oxo complexes, a very important question is whether a double bond is formed between the metal center and the oxo ligand or if the oxo ligand has a radical character in a metal–oxyl electronic structure.[3,4] The radical character of the oxo ligand is crucial to evaluate the reactivity in hydrogen-atom-abstraction from a substrate.[5] Among metal–oxo complexes, Ru^{IV}=O complexes have been a category of the most intensively investigated, owing to the high performance in catalytic oxidation reactions of not only organic substrates but also water.[6–9] Ru^{IV}=O complexes are formed through proton-coupled electron-transfer (PCET) oxidation of the corresponding Ru^{II}–aqua complexes and they also oxidize C–H bonds of substrates through a PCET mechanism.[10] Despite plenty of studies on the properties and reactivity of Ru^{IV}=O complexes, Ru^{III}–oxyl (Ru^{III}–$O^{\bullet}$) complexes, which have a single σ-bond between the Ru ion and the oxyl ligand and bear an electronically equivalent structure of Ru^{IV}=O complexes, have yet to be accessed. In light of the "oxo-wall", which is located between Groups 8 and 9 in the periodic table as proposed and elucidated by Gray and co-workers,[3b] an octahedral d^4 Ru^{IV} ion should have an oxo ligand connected by a double bond: the Ru^{IV}=O structure is more stable than the Ru^{III}–$O^{\bullet}$ structure and no rational strategy has been established to stabilize the Ru^{III}–$O^{\bullet}$ structure.[5,11,12] In this study, we employed a tridentate ligand (H-BPIm)[13] including an *N*-heterocyclic carbene (NHC) moiety, which exerts strong σ-donation and *trans* influence to form a Ru^{III}–$O^{\bullet}$ complex, and revealed the reactivity of the Ru^{III}–$O^{\bullet}$ complex in oxidation of organic substrates.

Syntheses of $[Ru^{II}Cl(BPIm)(bpy)]^+$ (**1**) and $[Ru^{II}(BPIm)(bpy)(OH_2)]^{2+}$ (**2**) are described in Scheme 1 and the details are given in the Supporting Information. Characterization of **1** and **2** was conducted with ^{1}H NMR spectroscopy (Figure S1), ESI-TOF-MS spectrometry (Figure S2), elemental analysis and X-ray crystallography. The crystal structures of **1**·Cl (Figure S3) and **2**·$(ClO_4)_2$ (Figures 1a and S4) indicate that the coordination manner of the BPIm ligand is not meridional but facial, which is consistent with the ^{1}H NMR spectra (Figure S1). The strong *trans* influence of the NHC ligand[14] was also clearly reflected on the crystal structure of

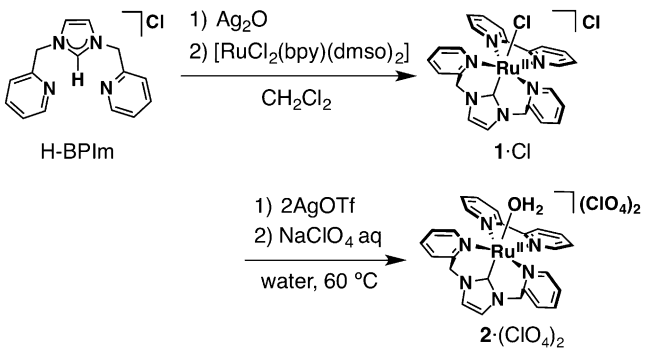

Scheme 1. Synthesis of a Ru(NHC)–aqua complex, **2**.

[*] Y. Shimoyama, Dr. T. Ishizuka, Dr. H. Kotani, Prof. Dr. T. Kojima
Department of Chemistry
Faculty of Pure and Applied Sciences
University of Tsukuba
1-1-1 Tennoudai, Tsukuba, Ibaraki 305-8571 (Japan)
E-mail: kojima@chem.tsukuba.ac.jp
Prof. Dr. Y. Shiota, Prof. Dr. K. Yoshizawa
Institute for Materials Chemistry and Engineering
Kyushu University
Motooka, Nishi-Ku, Fukuoka 819-0395 (Japan)
Dr. K. Mieda, Prof. Dr. T. Ogura
Picobiology Institute, Graduate School of Life Science
University of Hyogo, RSC-UH Leading Program Center
1-1-1 Kouto, Sayo-cho, Sayo-gun, Hyogo 679-5148 (Japan)
Dr. T. Okajima
Kyushu Synchrotron Light Research Center
8-7 Yayoigaoka, Tosu, Saga 841-0005 (Japan)
Prof. Dr. S. Nozawa
Photon Factory, Institute of Materials Structure Science
High Energy Accelerator Research Organization (KEK)
1-1 Oho, Tsukuba, Ibaraki 305-0801 (Japan)

Supporting information for this article can be found under: http://dx.doi.org/10.1002/anie.201607861.

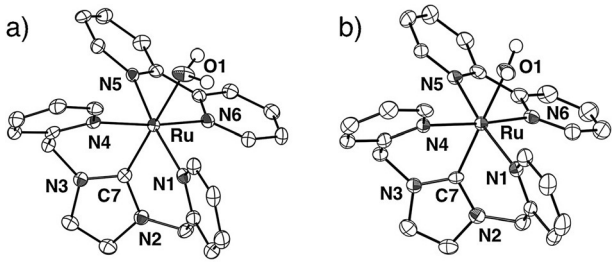

Figure 1. ORTEP drawings of **2**·$(ClO_4)_2$ (a) and **3**·$(ClO_4)_3$ (b) with 50% probability thermal ellipsoids. The counter anions and hydrogen atoms except those of the aqua ligands are omitted for clarity.

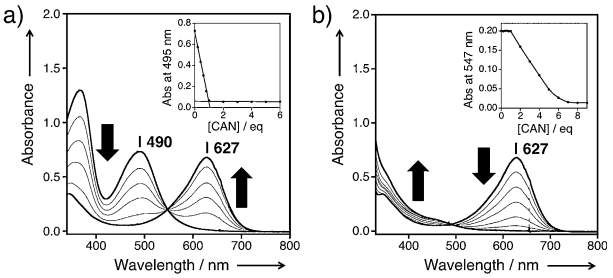

Figure 2. UV/Vis spectral titration of **2**·$(ClO_4)_2$ with CAN in HNO_3 aq (pH 0.6) at 277 K: a) 0–1 equiv, b) 1–8 equiv. Insets: absorbance changes at 495 nm for (a) and 547 nm for (b).

1·Cl. The bond distance of Ru–Cl in **1** is 2.5250(12) Å, which is longer than those of other Ru^{II}–Cl complexes (2.39–2.41 Å), having a pyridine ligand at the *trans* position of the Cl ligand.[15]

The redox behavior of **2**·$(ClO_4)_2$ in an aqueous solution was investigated by cyclic and square-wave voltammetries (CV and SWV) at room temperature. At pH 2.5, which was controlled with addition of $HClO_4$ to the aqueous solution of **2**·$(ClO_4)_2$, the CV showed a reversible redox wave at +0.86 V vs. NHE and a broad irreversible oxidation wave at +1.6 V vs. NHE (Figure S5). In the Pourbaix diagram, the potential of the first redox process showed no dependence on the solution pH (Figure S6). On the other hand, the potential of the second oxidation step lowered as the solution pH increased, with a slope of −108 mV/pH in the acidic region, indicating that the first redox step should be a 1 e^- process and the second oxidation should be a 1 e^-/2 H^+ process.[16] Therefore, the first wave was assigned to the oxidation of **2** to form $[Ru^{III}(BPIm)(bpy)(OH_2)]^{3+}$ (**3**) (Scheme 2). The assignment was a UV/Vis titration experiment of **2** with $(NH_4)_2$-$[Ce^{IV}(NO_3)_6]$ (CAN) (Figure 2a), ^{1}H NMR and ESR spectroscopies, and single-crystal X-ray crystallography.

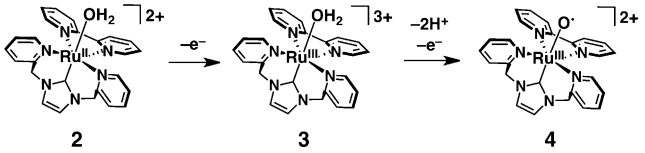

Scheme 2. Oxidation reaction of **2**.

Upon addition of CAN to an aqueous solution of **2**·$(ClO_4)_2$, whose pH was set to 0.6 with addition of nitric acid, the absorption band at 490 nm decreased and instead a new absorption band at 627 nm arose with an isosbestic point at 547 nm (Figures 2a and S8a). The change was saturated by addition of 1 equiv of CAN; the solution color changed from orange to blue. The absorption band at 627 nm was assigned to the LMCT transition from the NHC ligand to the Ru^{III} center in **3** using TD-DFT calculations (Figure S9). The ^{1}H NMR spectrum of **3** showed relatively broad signals in the range from −25 to 20 ppm, reflecting the paramagnetic character of **3** (Figure S10b). The ESR spectrum of **3** in water at 5 K exhibited a signal at $g_\perp = 2.419$ and $g_\parallel = 1.586$ (Figure S11). Thus, the root mean square of *g*-values, $\langle g \rangle$, was determined to be 2.177, which was a typical $\langle g \rangle$ value for Ru^{III} complexes ($S = 1/2$): approximately 2.2.[17] In the crystal structure of **3**·$(ClO_4)_3$ (Figure 1b), three perchlorate ions were included as counter anions. The bond length between the Ru center and the oxygen atom of the aqua ligand was shortened in **3**·$(ClO_4)_3$ (2.099(4) Å) as compared to that in **2**·$(ClO_4)_2$ (2.119(3) Å), reflecting the increase in the valence number of the Ru center from +2 to +3 (Table S2).

Further addition of CAN to the aqueous solution of **3** induced decrease of the absorption band at 627 nm with an isosbestic point at 495 nm (Figures 2b and S8b). The absorbance change was completed with addition of over 7 equiv of CAN (Figure 2b, inset). This can be ascribed to the high second-oxidation potential of **2** at +1.6 V vs. NHE, which is comparable to the reduction potential of CAN in an acidic aqueous solution (+1.61 V vs. NHE);[18] thus, the oxidation of **3** with CAN to give complex **4** requires addition of excess CAN to complete the reaction. According to the Pourbaix diagram of **2** (Figure S6), the oxidation of **3** to afford **4** should be a 1 e−/2 H^+ process. ^{1}H NMR spectral titration of **3** with CAN exhibited signals ascribable to a different paramagnetic species from **3** (Figure S10c) in a wider range of −35 to 30 ppm as compared to those of **3** ($S = 1/2$), suggesting that complex **4** should be in the $S = 1$ spin state.[19]

Further characterization of **4** was performed with ESI-TOF-MS spectrometry and resonance-Raman (rR) spectroscopy. The ESI-TOF-MS spectrum of **4**, which was derived from the oxidation of **2** by CAN in $H_2{}^{16}O$ and diluted with CH_3CN, showed a peak cluster of a divalent cation at $m/z =$ 262.01, which was assigned to $[Ru(^{16}O)(BPIm)(bpy)]^{2+}$ (calcd. 262.04); with use of $H_2{}^{18}O$ as the solvent in place of $H_2{}^{16}O$, the peak cluster shifted to $m/z = 263.02$ by substitution of ^{16}O with ^{18}O (Figure S13). The rR spectrum of **4** in an acidic aqueous solution (pH 4.0) at 276 K exhibited a Raman scattering derived from the Ru–O bond at 732 cm^{-1}; the use of $H_2{}^{18}O$ caused a low-energy shift of the signal to 696 cm^{-1} (Figure 3a). The isotope shift ($\Delta\nu$) was 36 cm^{-1}, which was consistent with the theoretical value ($\Delta\nu_{calc} = 36$ cm^{-1}). The energy value of the stretching band of the Ru–O bond was significantly lower than those of Ru^{IV}=O bonds reported to date ($\nu = 780$–833 cm^{-1}).[9,20] Additionally, the experimental value is close to that obtained from the DFT calculations on the Ru^{III}–O$^\bullet$ structure of **4** in the triplet state ($\nu = 767$ cm^{-1}; Figure S14).[21] The bond order of the Ru^{III}–O$^\bullet$ bond was also

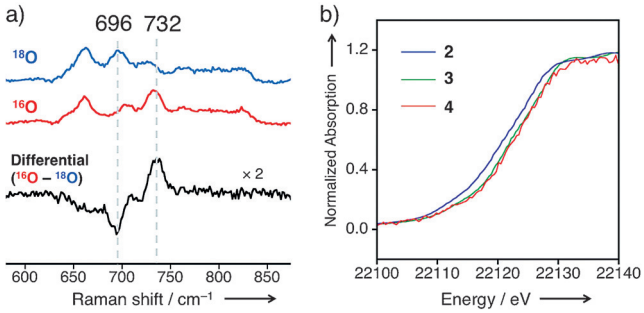

Figure 3. a) rR spectra of **4** in $H_2{}^{16}O$ (red) and in $H_2{}^{18}O$ (blue) at 276 K and the differential spectrum (black): Excitation wavelength: 441.6 nm. b) Normalized XANES spectra of **2** (blue), **3** (green), and **4** (red) at the Ru K-edge.

estimated to be 1.3 by DFT calculations (Figure S16). Therefore, the electronic structure of **4** can be assigned to the triplet Ru^{III}–O$^{\bullet}$ state, rather than a Ru^{IV}=O state. The valence number of the Ru center in **4** was confirmed by X-ray absorption near-edge structure (XANES) spectroscopy. The XANES spectra of **2**, **3**, and **4** at the Ru–K edge are shown in Figures 3b and S17. The energy at the half-height (E_{hh}) was gradually shifted to the higher region in the order of **2** < **3** < **4**; 22120.6 eV for **2**, 22122.1 eV for **3**, and 22122.6 eV for **4**. Comparing the E_{hh} values between **2** and **3**, the shift width is 1.5 eV and thus the increase of the valence number of the Ru center from +2 to +3 is adequately confirmed.[5c] In contrast, the shift width of the E_{hh} value from **3** to **4** is only 0.5 eV, and thus, the valence number of the Ru center in **4** should be close to +3, not to +4. Extended X-ray absorption fine structure (EXAFS) analysis on the aqueous solution of **4** allowed us to estimate the Ru–O bond of **4** to be 1.77(1) Å (Figure S18); although the bond length is in the range of Ru^{IV}=O bonds reported so far, in light of spectroscopic data and results of DFT calculations, we concluded that the electronic structure of **4** should be described as a Ru^{III}–O$^{\bullet}$ complex, rather than a Ru^{IV}=O complex.

Catalytic reactivity of **2** in oxidation of organic substrates was examined using CAN as a sacrificial oxidant in acidic water (pH ≈ 0.6) at 278 K, and the product yields after stirring for 24 h were determined by ^{1}H NMR spectroscopy (Tables 1 and S3).[22,23] In the case of oxidation of 2-propanol and cyclohexanol, the 2 e$^-$ oxidation proceeded to give acetone and cyclohexanone in 96% and 82% yields, respectively (entries 1 and 2). 4-Nitrobenzyl alcohol was also oxidized to 4-nitrobenzaldehyde (entry 3).[24] Sodium ethylbenzene sulfonate underwent 4e$^-$ oxidation to afford the corresponding acetophenone derivative with a relatively low yield (entry 4). It should be noted that benzaldehyde and the derivative were also oxidized to give the corresponding benzoic acids (entries 5 and 6); however, benzaldehyde and the derivatives are generally difficult to be oxidized with Ru^{IV}=O complexes.[9,25] This indicates the higher reactivity of the electronically equivalent Ru^{III}–O$^{\bullet}$ species **4** as the active species in C–H oxidation than Ru^{IV}=O species.[26] Terminal and internal alkenes gave the corresponding diols, which should be derived from cleavage of the epoxides under the strongly acidic conditions (entries 7 and 8).

Table 1: Summary of Product Yields (%) and Turnover Numbers of the Catalytic Oxidation Reactions with **2**.[a]

Entry	Substrate	Product	Yield [%]	TON[b]
1			96	230
2	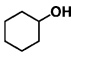		82	206
3[c]	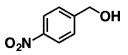	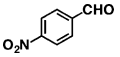	28[d]	69
4	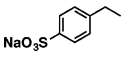	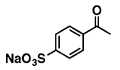	33	75
5	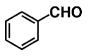	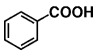	42	102
6	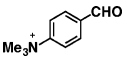	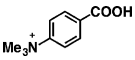	37	69
7	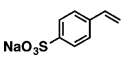	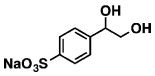	63	116
8	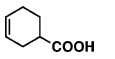	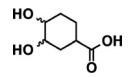	11:4[e]	27:8

[a] Reactions were performed under air at pH ≈ 0.6 and 278 K. [Substrate] = 34 mM, [CAN] = 75 mM, [**2**] = 0.14 μM, reaction time = 24 h. [b] TON = [Product]/[Catalyst]. [c] The reaction time was 1 h. See Ref. [24]. [d] As a byproduct, 4-nitro-benzoic acid was also obtained in 5% yield. [e] Product ratio of *cis*:*trans* diols.

To gain mechanistic insights into the oxidation process of benzaldehyde, kinetic studies were performed. The catalytic oxidations of benzaldehyde were performed in D_2O (pD ≈ 1) in the presence of CAN (0.31 M) and various concentration of **2**·$(ClO_4)_2$ (0.014–0.28 mM) at 283 K. The progress of the reaction was monitored by the ^{1}H NMR spectroscopy.[27] The initial rates, v_0, were determined with the slope of time-course of benzoic acid formation. On the basis of the dependence of v_0 on the concentration of **2**, the rate constant of the catalysis, $k_{cat}{}^{H}$, was determined to be 1.2 M^{-1}s^{-1} (Figure S20). The kinetic isotope effect (KIE) was also examined using deuterated benzaldehyde, PhCDO, under the same catalytic conditions. The $k_{cat}{}^{D}$ value was also determined to be 0.15 M^{-1}s^{-1} (Figure S21). Thus, the KIE value ($k_{cat}{}^{H}/k_{cat}{}^{D}$) was 8.0, indicating that hydrogen atom abstraction from the formyl group is involved in the rate-determining step of the oxidation reaction. A Hammett plot was generated by using other four benzaldehyde derivatives having various substituents at the *para* position to demonstrate that there was no dependence of the initial rate on the substituents ($\rho = -0.07$; Figure 4). Such large KIE and small ρ values have also been observed in galactose oxidase[29] and its model complex.[30] The results indicate that any polarized transition state, which has been suggested for the benzaldehyde oxidation with a Ru^{IV}=O complex ($\rho = -0.65$),[31] is not involved in the hydrogen-atom-abstraction process by **4**, and the oxidation of benzaldehyde does not proceed through a nucleophilic pathway. In the present catalytic reactions, benzaldehyde derivatives are oxidized through a pure hydrogen-atom-transfer mechanism. Therefore, we conclude that the Ru^{III}–O$^{\bullet}$ complex (**4**) bears a strong oxyl radical character.

In conclusion, we have succeeded in the formation and characterization of a Ru^{III}–O$^{\bullet}$ complex, which is electronically

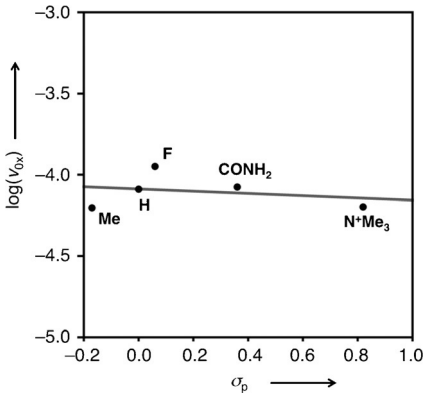

Figure 4. A Hammett plot of $\log(\nu_{0x})$ against σ_p for the oxidation of benzaldehyde derivatives in D_2O (pD ≈ 1) under 283 K in the presence of **2** (0.15 mM) as a catalyst. ν_{0x} refers to the initial rate for the oxidation of a benzaldehyde derivative having a substituent X at the *para* position. Concentration of a benzoic acid derivative was determined by integration values of the ^{1}H NMR signal for the *o*-H, based on an internal standard, DSS. The initial rates obtained, ν_{0x}, were 8.1×10^{-5} M min^{-1} for X = H ($\sigma_p = 0.0$), 6.3×10^{-5} M min^{-1} for X = Me ($\sigma_p = -0.17$), 1.1×10^{-4} M min^{-1} for X = F ($\sigma_p = 0.06$), 8.4×10^{-5} M min^{-1} for X = $CONH_2$ ($\sigma_p = 0.36$), and 6.4×10^{-5} M min^{-1} for X = N^+Me_3 ($\sigma_p = 0.82$), respectively. The Hammett parameters were obtained from the literature.[28]

equivalent to the corresponding Ru^{IV}=O species, with use of a tridentate NHC ligand. The Ru^{III}–O$^\bullet$ complex exhibits high reactivity in catalytic oxidation of organic substrates, including benzaldehyde derivatives in the presence of a Ce^{IV} complex as a sacrificial oxidant. In addition, the oxidation reaction includes hydrogen-atom abstraction from the substrate in a pure radical manner as the rate-determining step. Our strategy to elongate the metal–oxo bond by the strong *trans* influence of NHC ligands to reduce the π-bonding interaction between the metal center and the oxo ligand can provide a new category of metal–oxyl complexes with strong radical character toward efficient catalytic oxidation reactions of organic compounds. Exploring the application of the high reactivity of the Ru^{III}–O$^\bullet$ complex to further substrate oxidation is ongoing in our laboratory.

Acknowledgements

This work was supported by Grants-in-Aids (Nos. 24245011, 15H00915, 15H00890, and 15H00960) from the Japan Society of Promotion of Science (JSPS, MEXT) of Japan. XANES spectra measurement using synchrotron radiation was performed at BL07 of SAGA-LS (proposal No. 1512126F). EXAFS spectra were obtained using the beamline NW10A at PF-AR (proposal No. 2014S2-006). T.K. also appreciates financial supports from The Mitsubishi Foundation and Yazaki Memorial Foundation for Science and Technology. K. M. and T. O. are visiting scientists at RIKEN.

Keywords: catalysis · N-heterocyclic carbenes · oxyl radicals · ruthenium · substrate oxidation

How to cite: *Angew. Chem. Int. Ed.* **2016**, *55*, 14041 – 14045
Angew. Chem. **2016**, *128*, 14247 – 14251

[1] a) M. Costas, M. P. Mehn, M. P. Jensen, L. Que, Jr., *Chem. Rev.* **2004**, *104*, 939 – 986; b) B. Meunier, S. P. de Visser, S. Shaik, *Chem. Rev.* **2004**, *104*, 3947 – 3980.
[2] a) A. Kohen, J. P. Klinman, *Acc. Chem. Res.* **1998**, *31*, 397 – 404; b) W. Nam, *Acc. Chem. Res.* **2007**, *40*, 522 – 531.
[3] a) W. A. Nugent, J. M. Mayer, *Metal – Ligand Multiple Bonds*, Wiley, New York, **1988**; b) J. R. Winkler, H. B. Gray, *Struct. Bonding (Berlin)* **2012**, *142*, 17 – 28.
[4] a) I. Kretzschmar, A. Fiedler, J. N. Harvey, D. Schröder, H. Schwarz, *J. Phys. Chem. A* **1997**, *101*, 6252 – 6264; b) M. Baik, X. Yang, *J. Am. Chem. Soc.* **2006**, *128*, 7476 – 7485.
[5] a) T. Kojima, K. Hayashi, S. Iizuka, F. Tani, Y. Naruta, M. Kawano, Y. Ohashi, Y. Hirai, K. Ohkubo, Y. Matsuda, S. Fukuzumi, *Chem. Eur. J.* **2007**, *13*, 8212 – 8222; b) F. Neese, S. Ye, *Proc. Natl. Acad. Sci. USA* **2011**, *108*, 1228 – 1233; c) N. Planas, L. Vigara, C. Cady, P. Miró, P. Huang, L. Hammarström, S. Styring, N. Leidel, H. Dau, M. Haumann, L. Gagliardi, C. J. Cramer, A. Llobet, *Inorg. Chem.* **2011**, *50*, 11134 – 11142.
[6] a) R. A. Binstead, M. E. McCuire, A. Dovletoglou, W. K. Seok, L. E. Roecker, T. J. Meyer, *J. Am. Chem. Soc.* **1992**, *114*, 173 – 186; b) J. J. Concepcion, J. W. Jurss, J. L. Templeton, T. J. Meyer, *J. Am. Chem. Soc.* **2008**, *130*, 16462 – 16463.
[7] a) E. Masllorens, M. Rodríguez, I. Romero, A. Roglans, T. Parella, J. Benet-Bichholz, M. Poyatos, A. Llobet, *J. Am. Chem. Soc.* **2006**, *128*, 5306 – 5307; b) R. Staehle, L. Tong, L. Wang, L. Duan, A. Fischer, M. S. G. Ahlquist, L. Sun, S. Rau, *Inorg. Chem.* **2014**, *53*, 1307 – 1319.
[8] a) M. Dakkach, A. Atlamsani, T. Parella, X. Fontrodona, I. Romero, M. Rodríguez, *Inorg. Chem.* **2013**, *52*, 5077 – 5087; b) M. Dakkach, X. Fontrodona, T. Parella, A. Atlamsani, I. Romero, M. Rodríguez, *Adv. Synth. Catal.* **2011**, *353*, 231 – 238.
[9] a) Y. Hirai, T. Kojima, Y. Mizutani, Y. Shiota, K. Yoshizawa, S. Fukuzumi, *Angew. Chem. Int. Ed.* **2008**, *47*, 5772 – 5776; *Angew. Chem.* **2008**, *120*, 5856 – 5860; b) S. Ohzu, T. Ishizuka, Y. Hirai, H. Jiang, M. Sakaguchi, T. Ogura, S. Fukuzumi, T. Kojima, *Chem. Sci.* **2012**, *3*, 3421 – 3431.
[10] a) J. J. Warren, T. A. Tronic, J. M. Mayer, *Chem. Rev.* **2010**, *110*, 6961 – 7001; b) D. R. Weinberg, C. J. Gagliardi, J. F. Hull, C. F. Murphy, C. A. Kent, B. C. Westlake, A. Paul, D. H. Ess, D. G. McCafferty, T. J. Meyer, *Chem. Rev.* **2012**, *112*, 4016 – 4093.
[11] A ruthenium(II) – oxyl complex has been reported by Tanaka and co-workers: K. Kobayashi, H. Ohtsu, T. Wada, T. Kato, K. Tanaka, *J. Am. Chem. Soc.* **2003**, *125*, 6729 – 6739.
[12] Introduction of a strongly σ-donating ligand at the *trans* position to an oxo ligand is known to weaken the M=O bond and increase the spin density of the terminal oxygen atom. See: Ref. [5b].
[13] A. M. Magill, D. S. McGuiness, K. J. Cavell, G. J. P. Britovsek, V. C. Gibson, A. J. P. White, D. J. Williams, A. H. White, B. W. Skelton, *J. Organomet. Chem.* **2001**, *617*, 546 – 560.
[14] S. Fantasia, J. L. Petersen, H. Jacobsen, L. Cavallo, S. P. Nolan, *Organometallics* **2007**, *26*, 5880 – 5889.
[15] a) S. Ohzu, T. Ishizuka, H. Kotani, T. Kojima, *Chem. Commun.* **2014**, *50*, 15018 – 15021; b) H. Tseng, R. Zong, J. T. Muchkerman, R. Thummel, *Inorg. Chem.* **2008**, *47*, 11763 – 11773.
[16] The broadness and relatively large current of the second oxidation wave can be ascribed to catalytic oxygen evolution owing to water oxidation. See Figure S7.
[17] Y. Pushkar, D. Moonshiram, V. Purohit, L. Yan, I. Alperovich, *J. Am. Chem. Soc.* **2014**, *136*, 11938 – 11945.
[18] V. Nair, A. Deepthi, *Chem. Rev.* **2007**, *107*, 1862 – 1891.
[19] The ESR spectrum of **4** exhibited a signal at $g = 4.31$ ($\Delta m_s = \pm 2$), indicating the triplet state (Figure S12).
[20] H. Yamada, T. Koike, J. K. Hurst, *J. Am. Chem. Soc.* **2001**, *123*, 12775 – 12780.

[21] Single-point energy calculations were performed on the open-shell triplet, open-shell singlet, and closed-shell singlet states for the DFT-optimized structure of **4**. The triplet state was more stable than the singlet states (Figure S15). The bonding and antibonding orbitals related to the Ru–O bond are shown in Figure S16.
[22] As control experiments, we examined the reactions of the substrates listed in Table 1 with CAN under the same reaction conditions except in the absence of **2**·$(ClO_4)_2$. See Table S4.
[23] During the reviewing process, a referee suggested a nitrate effect on the oxidation reactions catalyzed by **2** (J. A. Stull, R. D. Britt, J. L. McHale, F. J. Knorr, S. V. Lymar, J. K. Hurst, *J. Am. Chem. Soc.* **2012**, *134*, 19973); however, the catalytic reactivity of **2** in the substrate oxidation, in which cerium(IV) sulfate was used as a sacrificial oxidant in the aqueous solution acidified with H_2SO_4, was almost the same as that with CAN in HNO_3 aq. Therefore, the nitrate effect was not found in the present catalytic system. See Table S5.
[24] After 24 h, most of 4-nitrobenzyl alcohol was oxidized by CAN even in the absence of a catalyst. Therefore, the catalytic oxidation of 4-nitrobenzyl alcohol was performed for 1 h.
[25] A. Gerli, J. Reedijk, M. T. Lakin, A. L. Spek, *Inorg. Chem.* **1995**, *34*, 1836 – 1843.
[26] As supporting evidence that complex **4** is the active species of the catalytic substrate oxidation by **2**, 10 equiv of 2-propanol was added to the solution of **4** in the presence of 10 equiv CAN in acidified D_2O. Then, the paramagnetic ^1H NMR signals of **4** decayed very quickly due to the reaction with 2-propanol, in comparison with the self-decomposition of **4** in the absence of substrates (Figure S19). The product of 2-propanol oxidation was confirmed to be acetone even under the concentrated conditions.
[27] See the Supporting Information.
[28] C. Hansch, A. Leo, R. W. Taft, *Chem. Rev.* **1991**, *91*, 165 – 195.
[29] M. M. Whittaker, J. W. Whittaker, *Biochemistry* **2001**, *40*, 7140 – 7148.
[30] Y. Wang, J. L. DuBois, B. Hedman, K. O. Hodgson, T. D. P. Stack, *Science* **1998**, *279*, 537 – 540.
[31] W. K. Seok, T. J. Meyer, *Inorg. Chem.* **2005**, *44*, 3931 – 3941.

Received: August 12, 2016
Revised: September 15, 2016
Published online: October 6, 2016

